Coral microbiomes are structured by environmental gradients in deep waters

Samuel A. Vohsen[1,2]* and Santiago Herrera[1,2]*

Abstract

Background Coral-associated microbiomes vary greatly between colonies and localities with functional consequences on the host. However, the full extent of variability across the ranges of most coral species remains unknown, especially for corals living in deep waters which span greater ranges. Here, we characterized the microbiomes of four octocoral species from mesophotic and bathyal deep-sea habitats in the northern Gulf of Mexico, *Muricea pendula, Swiftia exserta, Callogorgia delta,* and *Paramuricea biscaya,* using 16S rRNA gene metabarcoding. We sampled extensively across their ranges to test for microbiome differentiation between and within species, examining the influence of environmental factors that vary with depth (53–2224 m) and geographic location (over 680 m) as well as the host coral's genotype using RAD-sequencing.

Results Coral microbiomes were often dominated by amplicon sequence variants whose abundances varied across their hosts' ranges, including symbiotic taxa: corallicolids, *Endozoicomonas*, members of the *Mollicutes*, and the BD1-7 clade. Coral species, depth, and geographic location significantly affected diversity, microbial community composition, and the relative abundance of individual microbes. Depth was the strongest environmental factor determining microbiome structure within species, which influenced the abundance of most dominant symbiotic taxa. Differences in host genotype, bottom temperature, and surface primary productivity could explain a significant part of the microbiome variation associated with depth and geographic location.

Conclusions Altogether, this work demonstrates that the microbiomes of corals in deep waters vary substantially across their ranges in accordance with depth and other environmental conditions. It reveals that the influence of depth on the ecology of mesophotic and deep-sea corals extends to its effects on their microbiomes which may have functional consequences. This work also identifies the distributions of microbes including potential parasites which can be used to inform restoration plans in response to the Deepwater Horizon oil spill.

Keywords Mycoplasma, Oceanoplasma, Deep-sea, Mesophotic, Microbial biogeography, Seascape ecology

*Correspondence:
Samuel A. Vohsen
sav419@lehigh.edu
Santiago Herrera
santiago.herrera@lehigh.edu
[1] Department of Biological Sciences, Lehigh University, Bethlehem, PA, USA
[2] Lehigh Oceans Research Center, Lehigh University, Bethlehem, PA, USA

Background

Shallow-water, reef-building corals are well known for associating with microalgae in the family *Symbiodinaceae*. All corals, including those in the deep sea, form associations with diverse groups of bacteria [1], archaea [2, 3], unicellular eukaryotes [4], and viruses [5], collectively called the coral microbiome. Many members of the microbiome are important to the health of corals, either as pathogens [6] or providing sources of nutrition [7, 8].

Common coral associates include eukaryotic apicomplexans of the order *Corallicolida* [9–13] and the bacterial

genera *Mycoplasma* [14–19] and *Endozoicomonas* [1, 20–22]. These taxa are among the most-studied coral-associated microbes and exhibit many indications of a close relationship with their coral hosts. *Endozoicomonas* form dense aggregates in coral tissue [23, 24] and conduct activities relevant to the corals such as producing vitamins [25, 26], degrading dimethylsulfoniopropionate [27], and cycling phosphorus [28]. While widely assumed to be mutualists, some have proposed that *Endozoicomonas* may be parasitic or pathogenic since they are generally more abundant in coral species that are less capable of adapting to environmental change [29]. Similarly, corallicolids and *Mycoplasma* are commonly found in many coral species and reside within or on coral tissue [10, 18, 30–33]. Most apicomplexans [34] and *Mycoplasma* spp. [35] are parasites or pathogens. However, those found in corals have not been associated with pathology or reduced fitness [31, 36]. While these common coral associates have been the focus of extensive research, we have a limited understanding of the variability of coral-microbe associations.

The compositions of coral microbiomes can vary substantially between and within coral species and across geographic locations [20, 37, 38]. The genotype of the host coral underlies some of this variation [37, 39, 40], as do environmental factors such as water temperature [41], habitat type [42], and pollution levels [41, 43]. These factors can differ across the ranges of coral species, yet the scope of most studies is limited to a narrow selection of a species' known geographic or depth range. Further, most studies have focused on shallow-water corals, mainly scleractinians, and to a lesser degree on black corals and the more diverse octocorals [32, 38, 44]. Overall, the extent of coral microbiome variability is likely underestimated.

Variations in coral microbiomes can have functional implications. In shallow-water scleractinian species, certain microbial assemblages are associated with increased thermal tolerance [45–47]. Microbiome variation could be significant for mesophotic and deep-sea corals (those living deeper than 50 m) because they often have wider depth and geographic ranges than shallow-water species [48].

Mesophotic and deep-sea corals support diverse and abundant biological communities in Earth's largest biome [49–53]. Most are heterotrophic because they live beyond the reach of sunlight sufficient for photosynthesis. Like shallow-water corals, they face human-induced stressors such as ocean warming, acidification, pollution, and ecosystem destruction [54–57]. In the mesophotic zone and deep sea, octocorals comprise approximately 70% of all coral species [58]. A comprehensive characterization of microbiome variation in octocorals across their geographic ranges is needed to understand the diversity and ecological roles of microbiomes in deep-water habitats.

Mesophotic and deep-sea octocorals occur worldwide along continental margins and seamounts, over a wide depth range down to at least 8000 m [48, 59]. Light intensity, oxygen concentration, temperature, pressure, pH, salinity, food availability, and habitat structure vary with depth and geography. All these factors combine to strongly influence the ecology and evolution of marine animals [60–63]. Thus, factors that vary with depth and geographic location likely drive microbiome variation in mesophotic and deep-sea octocorals as well.

Here we test the hypotheses that the microbiomes of mesophotic and deep-sea octocorals vary significantly across their ranges in correlation with environmental factors and host genotype. We characterized the microbiomes of the mesophotic octocorals *Muricea pendula* and *Swiftia exserta,* and the deep-sea octocorals *Callogorgia delta* and *Paramuricea biscaya* across their known depth and geographic ranges in the northern Gulf of Mexico (Fig. 1). All of these corals are dominant foundation species in their respective communities and are the focus of restoration efforts because at least three suffered mortality during the Deepwater Horizon oil spill [54, 55, 64–66]. Understanding the geographic variation of their associated microbes is essential to understanding the ecology of coral ecosystems and can also inform restoration plans.

Methods
Sample collection
Octocorals were sampled between 2009 and 2019 from multiple sites across their ranges in the northern Gulf

(See figure on next page.)
Fig. 1 Sampling sites and their environmental and coral genotypic makeup. **A** In situ images of the octocoral species in this study. **B** Geographic map displaying sampling locations in the Northern Gulf of Mexico (BOEM bathymetry). The mean depth of all samples from a site is reported next to each site name in meters. Sites are colored based on which coral species were sampled: light gray = *Muricea pendula,* red = *Swiftia exserta,* blue = *Callogorgia delta,* yellow = *Paramuricea biscaya*. Images of *C. delta* and *P. biscaya* courtesy of the ECOGIG consortium. **C** Surface primary productivity of each sampling site displayed across longitude and colored by coral species sampled therein. **D** Bottom seawater temperature for each sampling site displayed across depth for each coral species. **E** UMAP projections of the genetic background of coral colonies based on RADseq data. Each point represents the genotype of a coral colony and is colored by depth
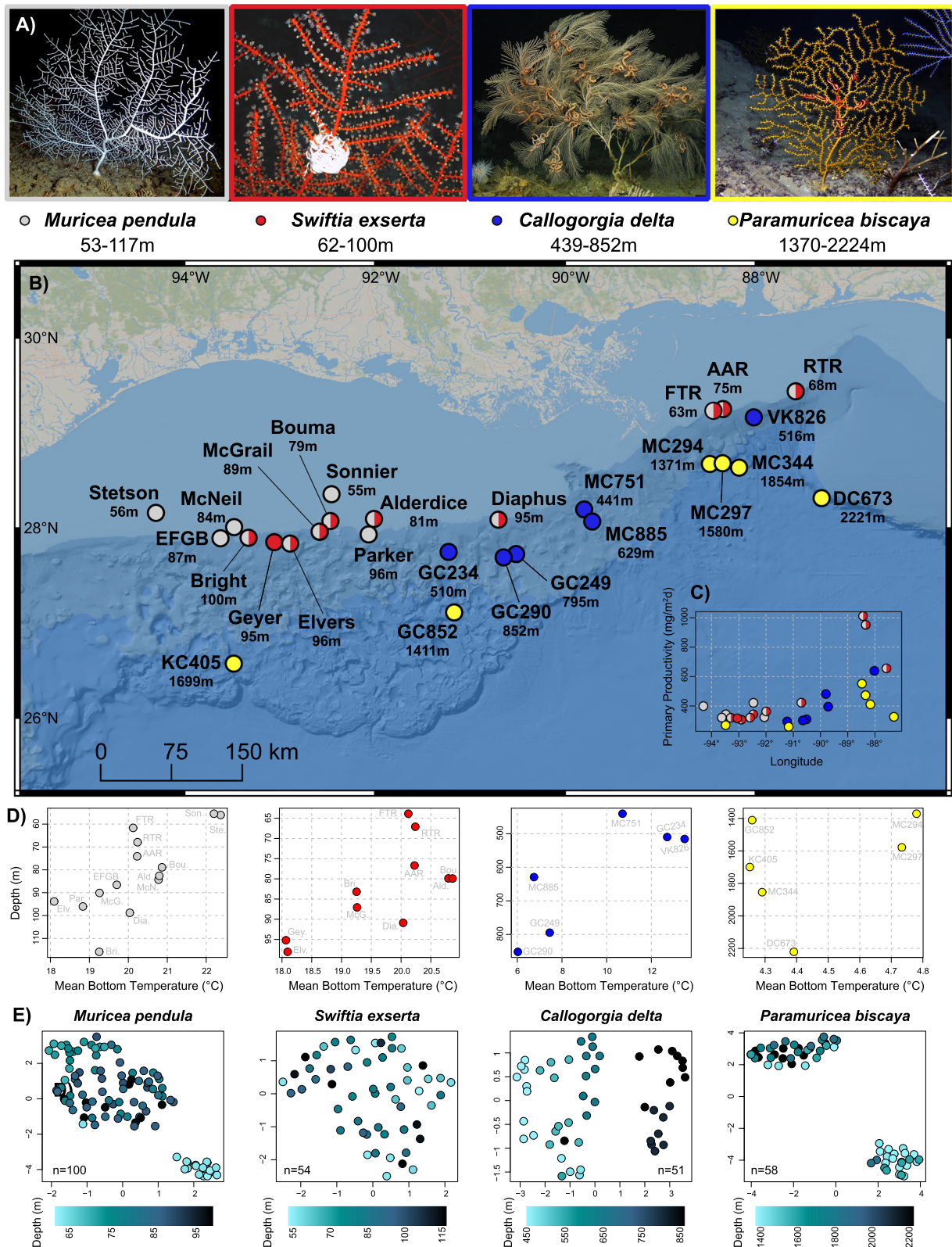
Fig. 1 (See legend on previous page.)

of Mexico using Remotely Operated Vehicles (ROVs). They were placed in temperature-insulated containers at the seafloor and processed immediately after each dive. Specimens of four species were collected including the mesophotic octocoral *Muricea pendula* (n = 140, 10 individuals per site, 14 sites spanning 34–690 km and 53–117 m in depth), the co-occurring octocoral *Swiftia exserta* (n = 100, 10 per site, 10 sites spanning 13–600 km and 62–100 m in depth), the upper-bathyal octocoral *Callogorgia delta* (n = 60, 10 per site, 6 sites spanning 14–350 km and 439–852 m in depth), and lower-bathyal octocoral *P. biscaya* (n = 60, 9–11 per site, 6 sites spanning 14–655 km and 1370–2224 m in depth). Details, including research cruise, time of collection, and preservation method for each sample, can be found in Table S1.

DNA purification
Whole DNA was purified using a modified salting-out procedure [67]. To standardize DNA concentrations and reduce the concentration of PCR inhibitors, we measured purified DNA concentrations on a Qubit 4.0 fluorometer with a qubit Broad Range assay and then diluted with TE buffer to 2 ng/µl for *Swiftia exserta*, 20 ng/µL for *Muricea pendula*, 10 ng/µL for *Callogorgia delta*, and 10-40 ng/µL for *P. biscaya*. DNA extracts of *C. delta* and *P. biscaya* that were less concentrated than these thresholds were not diluted. See Supplementary Methods in Additional File 1 for details.

Microbial metabarcoding
The hypervariable V1-V2 regions of the bacterial 16S rRNA gene were amplified following Vohsen et al. [9] using the universal primers 27F and 355R. PCR products were sent to the University of Illinois Chicago for library preparation and sequencing [68] on an Illumina Miseq platform in a single sequencing lane with 250 bp paired-end reads and V2 chemistry.

Raw sequence data were imported into *qiime2* [69] version 2021.2 and processed following Vohsen et al. [9] to create an amplicon sequence variant (ASV) table. Details can be found in the Supplementary Methods in Additional File 1.

Coral genotyping
To investigate the influence of the host's genotype on the microbiome, Restriction site-Associated DNA sequence (RADseq) data were obtained from a subset of coral colonies as described by Bracco et al. [61] and Galaska et al. [62]. In brief, DNA was sent to Floragenex Inc. (Eugene, OR) for RAD library preparation using the restriction enzyme, PstI, and sequencing on an Illumina HiSeq platform. Sequence reads were demultiplexed and quality-filtered using the *process_radtags* program in Stacks v2.1

[70]. Read clustering and single nucleotide polymorphism (SNP) calling were performed with DeNovoGBS v4.0.1 [71] for *C. delta* and *P. biscaya*, and with gstacks v2.1 [70] for *S. exserta* and *M. pendula* after mapping to genome assemblies for each. We excluded SNP loci that: (1) had more than 10% of missing data, (2) had a minor allele frequency smaller than 0.01, or (3) were not biallelic. We also excluded individuals that were missing data for > 10% of SNP loci for *S. exserta* and *M. pendula* and > 30% for *C. delta* and *P. biscaya* or were identified as clones with R package *poppr* v2.8.6 [72]. To reduce the dimensionality of the genetic data, a principal component analysis (PCA) was performed on the SNP data of each species separately (*S. exserta,* 23,869 SNPs, n = 54; *M. pendula,* 9,611 SNPs, n = 100; *C. delta*, 14,013 SNPs, n = 51 and *P. biscaya,* 7,293 SNPs, n = 58) using the R package *ade4* v1.7 [73]. The PCA axes were reduced to two dimensions using the uniform manifold approximation and projection method [74] using the R package *umap* v0.2.8. Genetic distances between individuals within species were calculated as pairwise allelic differences using the R package *poppr* v2.9.4.

Environmental variables
Publicly available satellite data and model-derived values for the Gulf of Mexico were obtained to evaluate the influence of environmental variables on coral microbiomes. The satellite-derived estimates of surface primary productivity (mg/m^{2}d), chlorophyll concentration (mg/m^3), inorganic suspended particulate matter concentration (g/m^3), and the particulate back-scattering coefficient at 443 nm (m^{-1}) were obtained from the Copernicus-GlobColour Global Ocean Colour biogeochemical dataset. Model-derived values were obtained for the depth of the surface mixed layer (m), bottom seawater temperature (°C), bottom seawater oxygen concentration (mL/L), bottom seawater salinity, and bottom current magnitude (m/s) from the HYbrid Coordinate Ocean Model (HYCOM). Both datasets comprised monthly means from Jan 2011 to Dec 2018 at 4 km grid resolution. The mean and standard deviation of monthly means for each variable were extracted at the sampling location of each coral colony. Only the mean bottom seawater temperature and surface primary productivity were retained for statistical analyses. Other variables were excluded from the analyses because they were strongly correlated, not substantially variable across sites, or were not justified by a priori hypotheses. See Tables S2, S3 for further details.

Statistical analyses
Rarefied microbial ASV richness was calculated for each coral colony using the *rarefy* function in the R package

vegan [75] v2.5.7 using the minimum library size (1220 reads) as the sampling depth following Hurlbert [76]. Pielou's evenness was calculated for each individual using the function *evenness* in the R package *microbiome* v1.16.0 [77]. Microbial community richness and evenness were compared between coral species and across sites using a Kruskal–Wallis rank-sum test followed by pairwise two-tailed Wilcoxon rank-sum tests with a Bonferroni-adjusted α-value using the functions *kruskal.test* and *wilcox.test* in the base R package *stats* v4.1.2. In addition, the effects of depth and longitude on richness and evenness were evaluated for each species using a multiple linear regression model (MLR) with depth and longitude as predictors and richness or evenness as response variables.

Permutational Analysis of Variance (PERMANOVA) [78] and distance-based Redundancy Analysis (dbRDA) [79] were performed to evaluate the influence of host species, depth, geography (site and longitude), bottom temperature, and surface primary productivity on microbiome compositions. Longitude was chosen to test for regional scale patterns across geography while sampling site was used as a finer scale variable. PERMANOVA and dbRDA analyses were performed using the R functions *adonis2*, *dbrda*, and *anova.cca* in the package *vegan* with Bray–Curtis dissimilarities on ASV proportions and 9,999 permutations. The results of both analyses were congruent so only the PERMANOVA results are discussed in the text. The details of each test are provided in Tables S4 and S5. In addition, the diversity among *Endozoicomonas* and corallicolids associated with *S. exserta* and *M. pendula* were analyzed individually using PERMANOVA to determine the influence of host species, depth, longitude, and site.

The effect of host genotype on microbiome dissimilarity was tested using Multiple Regression on distance Matrices (MRM) [80]. Bray–Curtis dissimilarities of 4th root-transformed ASV proportions were used as the response variable while geographic distances, host genetic distances, and Euclidean differences in depth, bottom temperature, and surface primary productivity were used as predictor variables. Geographic distances were calculated from latitude and longitude coordinates of each sample using the *distm* command in the R package *geosphere* with the Haversine function. MRM was conducted using the *MRM* command in the R package *ecodist* with 100,000 permutations.

Individual ASVs whose abundance differed along depth, longitude, and across sites were identified using Analysis of Compositions of Microbiomes with Bias Correction (ANCOM-BC) [81] using the R package *ancombc* v1.4.0. Two separate ANCOM-BC analyses were conducted on each species individually: (1) using both depth and longitude as explanatory variables and (2) a global analysis using sampling sites as groups. ASVs were excluded from the analysis if they were present in fewer than five individual corals (half the colonies sampled at a single site). The false discovery rate was controlled using the Benjamini–Hochberg method. The global analyses were repeated using each site as the reference. Only ASVs with a maximum q-value below α = 0.05 in all permutations were considered significantly different. These analyses were repeated on the family level to inform functional differences.

In order to account for differences in preservation method and sampling year, statistical analyses were repeated including those as explanatory variables. In addition, the same analyses were applied to a separate publicly available dataset of *C. delta* colonies from the same sites. Please see Additional File 1 and Tables S9 and S10 for further details demonstrating the consistency of results.

An analysis of homogeneity of multivariate dispersions between sites was performed for each species using the command *betadisper* with group centroids in the R package *vegan* (Table S12). Principal coordinates of each species were plotted showing centroid differences between sites (Fig. S8).

Results

Microbiomes are distinct among octocoral species.

The microbiomes of all four coral species were dominated by ASVs that represented more than 50% of the microbial community in at least one colony (Fig. 2B, Table S6). *M. pendula* had the greatest diversity of dominant ASVs, including two *Mycoplasma*, two *Marinoplasma*, an *Endozoicomonas*, an unclassified alphaproteobacterium, and a corallicolid apicomplexan. *S. exserta* hosted only two dominant ASVs: one classified as BD1-7 clade (*Spongiibacteraceae*) and another classified as *Mycoplasma*. Both *C. delta* and *P. biscaya* hosted three dominant ASVs. All three dominant ASVs in *C. delta* were recently described [30] as novel members of the class *Mollicutes*: two *Ca. Oceanoplasma* and one *Ca. Thalassoplasma*. The dominant ASVs in *P. biscaya* were classified as *Mycoplasma*, *Endozoicomonas,* and *Pseudoalteromonas.* Dominant ASVs belonging to the same taxon were given short identifiers (ex: M1, M2, S2) to distinguish which coral species they were associated with (first letter of coral genus) and the rank of abundance (1 being most abundant).

Each coral species had a distinct microbial community (Fig. 2A, B; Table S4A; PERMANOVA R^2 45%, $p \leq 10^{-4}$). All dominant ASVs were abundant in only one coral species and were rare (< 4%) in all others. The only exception was the corallicolid ASV M1 in *M. pendula* which was also abundant, but less so, in *S. exserta* along with
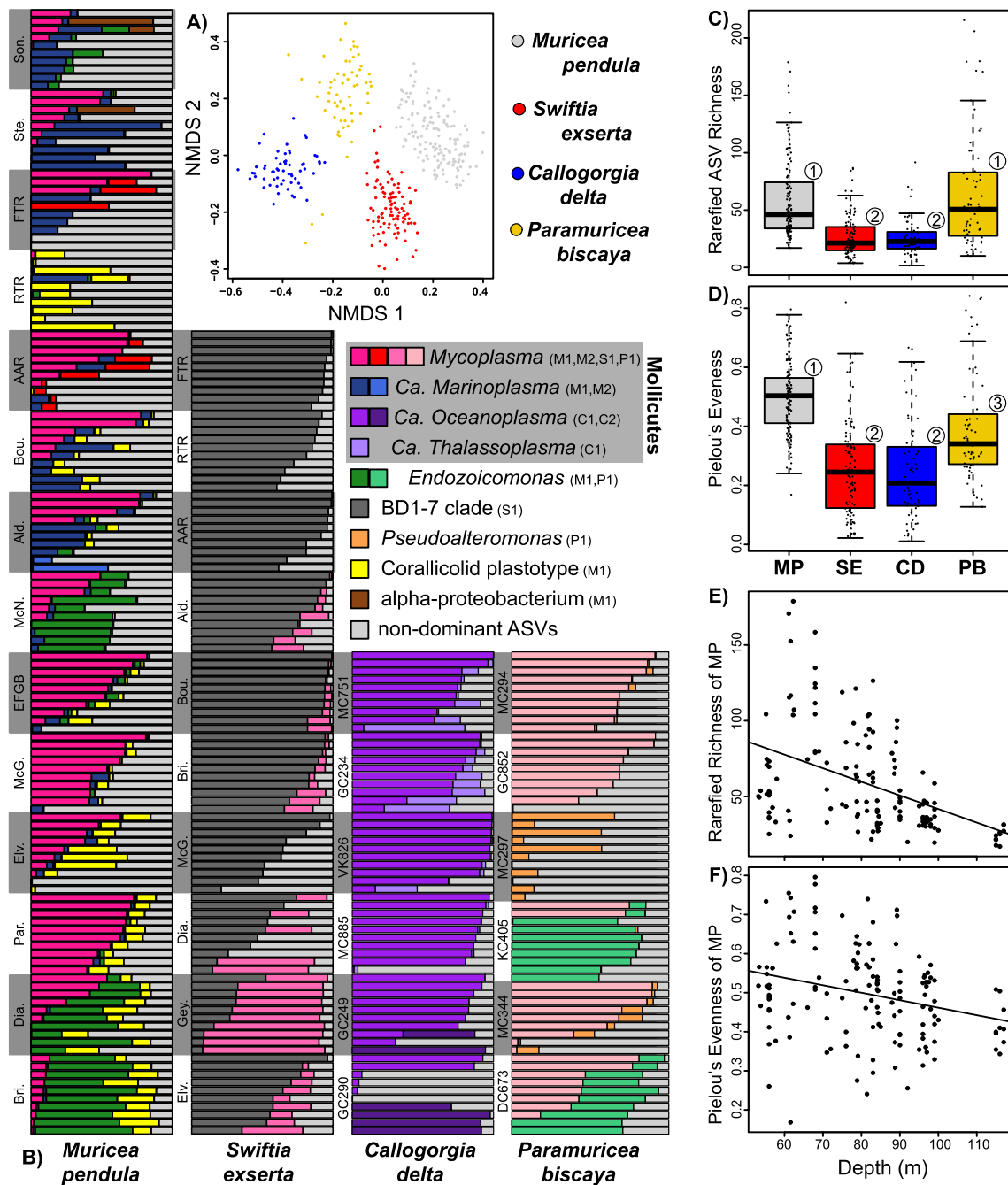
Fig. 2 Characterization of coral microbiomes. **A** Non-metric multidimensional scaling plot of microbiome compositions using Bray–Curtis dissimilarities of ASV proportions. **B** Barplots of dominant ASVs in each coral species. Each horizontal bar represents the relative abundance of ASVs in an individual coral colony which sum to 100%. Colonies are grouped by site which are sorted by depth. ASVs that comprised 50% or more in any sample are designated with different colors. All other ASVs are collapsed and shown in light gray. *Ca. Oceanoplasma* and *Ca. Thalassoplasma* were recently described by Vohsen et al. (2022). **C** Rarefied ASV richness and **D** Pielou's evenness between different coral species. MP = *Muricea pendula*, SE = *Swiftia exserta,* CD = *Callogorgia delta,* PB = *Paramuricea biscaya*. **E** Rarefied ASV richness and **F** Pielou's evenness in *Muricea pendula* with depth. Numbers over boxplots designate significantly different groups

other corallicolid ASVs. Coral species also differed in microbiome richness and evenness (Kruskal–Wallis rank-sum test, $p < 2.2 \times 10^{-16}$, Table S7A). The microbiomes of *M. pendula* and *P. biscaya* had higher rarefied ASV richness and Pielou's evenness than *S. exserta* and *C. delta* (Fig. 2C, D; Table S7A; post-hoc pairwise Wilcoxon rank-sum tests, $p \leq 5.4 \times 10^{-6}$).

Factors shaping microbiomes

The microbial communities of all coral species differed significantly across sites which accounted for 33–59% of the variation within species (Table S4B, PERMANOVA $p \leq 10^{-4}$). This variation was driven by significant trends across depth ($p \leq 10^{-4}$) and longitude ($p \leq 0.0251$), which simultaneously accounted for 11–17% and 3–12% of the variation, respectively, depending on coral species (Table S4C). The only exception was *C. delta,* whose microbial community composition was not significantly correlated with longitude. After accounting for depth and longitude, sampling site remained associated with a significant ($p \leq 0.016$) and substantial amount of additional variation (13–44%) for each coral species (Table S4D). However, sampling site no longer explained a significant amount of variation in *C. delta* after accounting for preservation method and sampling year (Table S9D).

Temperature decreased with depth and was associated with a significant amount of microbiome variation in all species (Fig. 1D; Table S4E; PERMANOVA $p \leq 0.0156$, 5–14%) except *P. biscaya* in which it was not tested due to low variation between sites (< 0.6 °C). However, this did not account for the entire structure with depth which retained a significant correlation with microbiome dissimilarity after accounting for temperature (Table S4E; PERMANOVA $p \leq 0.0006$, 4–9%, Table S4E). Similarly, surface primary productivity was higher in the east and could explain a significant amount of microbiome variation in all species except *C. delta* (Fig. 1C; Table S4F; PERMANOVA $p \leq 0.0154$, 1–7%). After accounting for primary productivity, longitude was still associated with a significant amount of variation (Table S4F; PERMANOVA $p \leq 0.0063$, 4–11%,).

Microbiome dissimilarity was significantly correlated with host genetic distances while controlling for covariates in *P. biscaya* (Table S8A, MRM $p = 0.006$) and weakly in *M. pendula* (Table S8A; MRM $p = 0.041$). In *C. delta,* genetic distance was strongly correlated with depth (Table S8B; Partial Mantel $p = 10^{-4}$) and was significantly correlated with microbiome dissimilarity when ignoring depth (Table S8C; MRM $p = 0.01$).

Microbiome patterns with depth

Depth was correlated with microbiome diversity in various ways. In *Muricea pendula,* both richness (Fig. 2E; MLR p = 6×10^{-6}) and evenness (Fig. 2F; MLR $p = 0.012$) decreased significantly with depth. The decrease in diversity in *M. pendula* was great enough that the average richness among colonies from the deepest sites was comparable to the richness observed in *S. exserta* and *C. delta* (Fig. S1 in Additional File 1). Conversely, both richness and evenness in *S. exserta* increased with depth (MLR $p \leq 6 \times 10^{-6}$), as did richness in *C. delta* (MLR $p = 0.038$).

The relative abundances of multiple microbial taxa strongly correlated with depth including many dominant taxa. In *M. pendula, Endozoicomonas* ASV M1 increased in abundance with depth and so did the total abundance of all *Endozoicomonas* ASVs (Fig. 3A, ANCOM-BC, $q = 4 \times 10^{-9}$, 10^{-12}). Similarly, the abundance of the dominant corallicolid ASV M1 increased with depth in *M. pendula* (ANCOM-BC, $q = 3 \times 10^{-57}$). This was also true for the total abundance of all corallicolid ASVs in *Muricea pendula* (Fig. 3B; ANCOM-BC $q = 6 \times 10^{-48}$) and *Swiftia exserta* (Fig. S2A in Additional File 1; ANCOM-BC $q = 7 \times 10^{-8}$). In contrast, other dominant ASVs decreased in abundance with depth: BD1-7 ASV S1 in *S. exserta* (Fig. 3E; ANCOM-BC, $q = 5 \times 10^{-5}$), *Ca. Marinoplasma* ASV M1 in *M. pendula* (Fig. 3C; ANCOM-BC, $q = 1 \times 10^{-7}$), and *Ca. Thalassoplasma* C1 in *C. delta* (Fig. 2B; $q = 2 \times 10^{-52}$).

Many other taxa that comprised a smaller proportion of the microbial community also differed with depth (Fig. 3D). *M. pendula* hosted many of these taxa and the majority decreased in abundance with depth (54/80 non-dominant ASVs and 36/42 families, ANCOM-BC $q \leq 0.05$). The most abundant of these non-dominant, depth-decreasing taxa included photosynthetic groups such as *Cyanobiaceae* and chloroplasts but also ASVs in the families *Spirochaetaceae, Helicobacteraceae, Flavobacteriaceae, Francisellaceae, Burkholderiaceae*, and unclassified bacteria that clustered with *Spirochaetia* and *Epsilonproteobacteria*. Together with the dominant *Ca. Marinoplasma* M1, these taxa averaged 70% of the microbial community among *M. pendula* colonies from the shallowest site (Sonnier Bank, 55 m) and decreased to a mean of 3% at the deepest site (Bright Bank, 116 m, Fig. 3D). Although many of these taxa were also detected in *S. exserta,* their abundances were either not significantly correlated with depth or increased with depth.

The composition of ASVs within microbial taxa also shifted with depth. For example, *Endozoicomonas* ASVs in *M. pendula* (Fig. 3F, Table S4G; PERMANOVA $p \leq 10^{-4}$) and corallicolids in *S. exserta* (Fig. S2K in Additional File 1; Table S4G, PERMANOVA $p = 0.0029$). Notably, *M. pendula* and *S. exserta* each hosted a unique corallicollid ASV at the deep site Elvers Bank (96 m). Similar depth transitions were also prevalent among the associates of *C. delta. Ca. Oceanoplasma* ASV C1 dominated the microbial community of most *C. delta* colonies from most sites except the deepest two sites (Fig. 2B, GC249 and GC290). At these sites, the closely related *Ca. Oceanoplasma* ASV C2 dominated some colonies. Shifts in ASVs were also seen among *Endozoicomonas* and *Shewanella* associates of *C. delta* (Fig. 3G, H, ANCOM-BC by ASV, $2 \times 10^{-38} \leq q \leq 0.002$). A single *Endozoicomonas* ASV was present in most colonies from all sites (Fig. 3G,
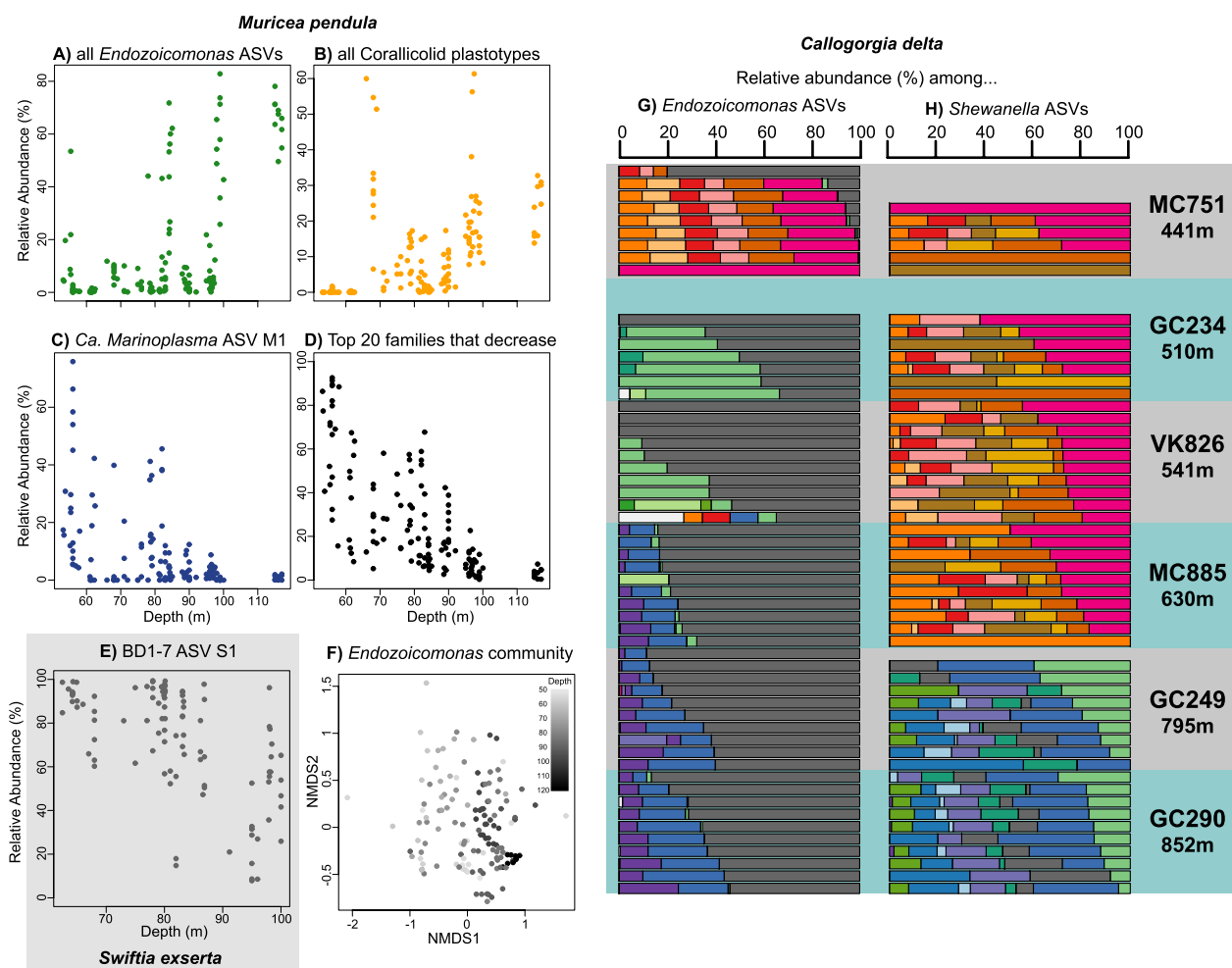
Fig. 3 Examples of depth patterns in coral microbiome composition. The relative abundances along depth in *Muricea pendula* of **A** the sum of all *Endozoicomonas* ASVs, **B** the sum of all corallicolid ASVs, **C** *Ca. Marinoplasma* ASV M1, **D** the sum of top 20 microbial families that decreased significantly with depth. **E** Relative abundance of BD1-7 ASV S1 with depth in *Swiftia exserta*. **F** NMDS ordination of *Endozoicomonas* communities in *M. pendula* showing patterns with depth. The community composition of **G** *Endozoicomonas* and **H** *Shewanella* communities in *Callogorgia delta*. Each horizontal bar is a single coral colony whose composition reflects the relative abundances of each ASV when restricted to only *Endozoicomonas* or *Shewanella* ASVs. Colors denote different ASVs. Colonies are arranged by site in order of increasing mean depth

gray bars), while other ASVs were mostly restricted between three depth zones. More strikingly, *Shewanella* communities between colonies from two depth zones (< 637 m and > 794 m) were completely non-overlapping, failing to share a single ASV (Fig. 3H).

Microbiome patterns with geography

Microbiome richness was higher in the east for both *M. pendula* and *S. exserta* (Table S7B; MLR $p < 2 \times 10^{-8}$). Multiple microbes exhibited differences in abundance across the geographic range of their host coral (Fig. 4A-F; ANCOM-BC, $9 \times 10^{-11} \leq q \leq 0.05$). *M. pendula* colonies from eastern sites had higher abundances of *Mycoplasma* ASV M2 and ASVs classified as *Endozoicomonas*,

corallicolids, BD1-7, *Spirochaetaceae, Alteromonas, Pseudoalteromonas, Pseudomonas, Marinobacter, Ruegeria, Caedibacter, Sphingomonadaceae*, and *Cyanobiaceae*. The mean total relative abundance of all ASVs that were more abundant in the east ranged between 0.8% and 26%, excluding the dominant *Mycoplasma* ASV M2 and dominant corallicolid ASV M1. Some of these same ASVs and related taxa were also more abundant in *S. exserta* in the east including *Pseudomonas, Pseudoalteromonas, Alteromonas, Ruegeria, Endozoicomonas, Cyanobiaceae*, BD1-7, and *Spirochaetaceae* (Additional File 3, ANCOM-BC $0.0018 \leq q \leq 0.05$).

Other *Cyanobiaceae, Mycoplasma,* and *Endozoicomonas* ASVs were more abundant in *M.*
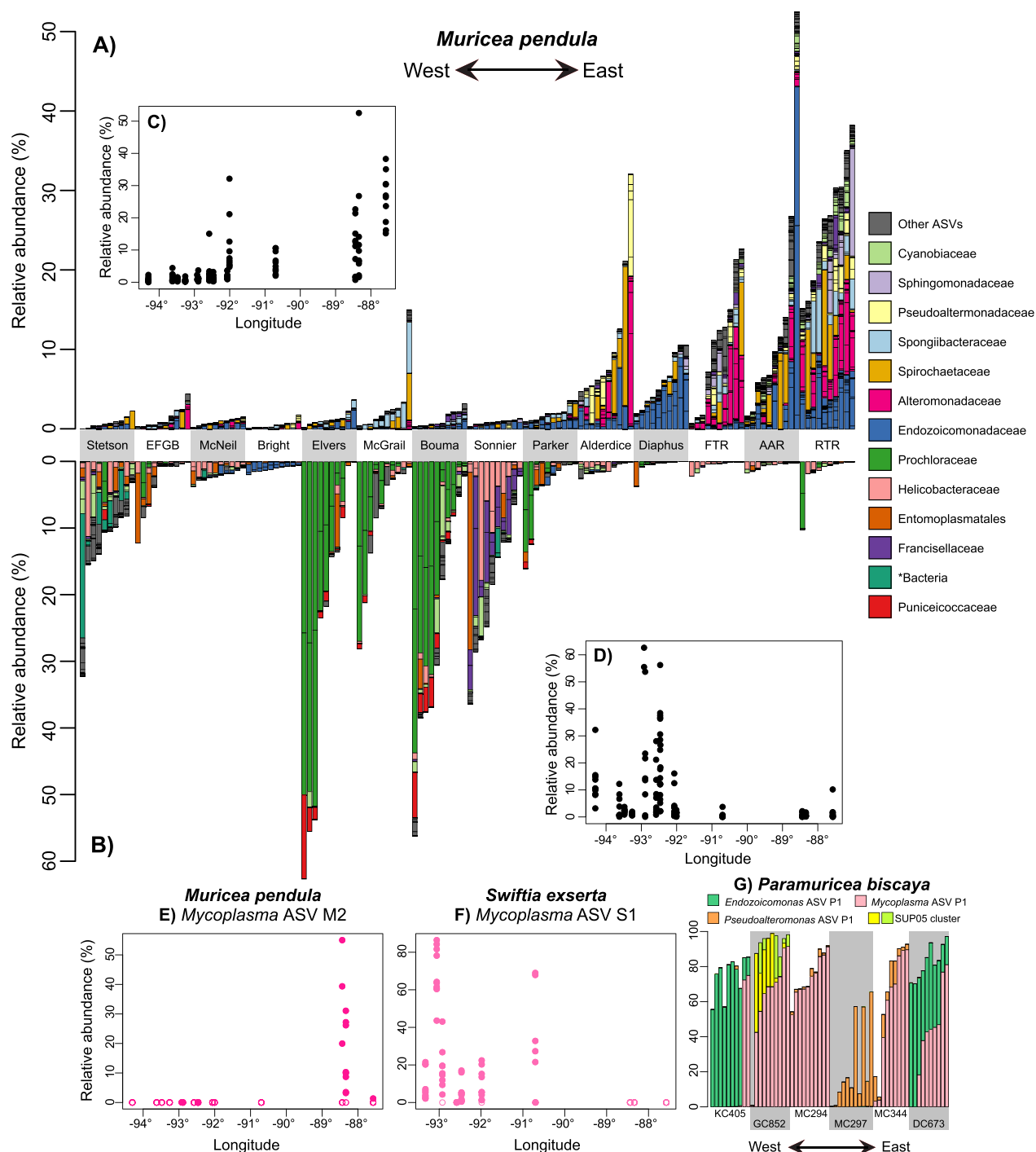
Fig. 4 Examples of geographic patterns in coral microbiome composition. Barplots of the relative abundance of microbial ASVs from *Muricea pendula* that **A** increased and **B** decreased from West to East across its range in the Northern Gulf of Mexico. ASVs are colored by family or other taxonomic level detailed in the legend. Each coral colony is represented by a vertical bar, and colonies are grouped by site sorted from westernmost to easternmost starting from the left. The total relative abundances of these ASVs are shown in **C** and **D** plotted against longitude to better reflect relative distances between sites. The relative abundance of **E** *Mycoplasma* ASV M1 in *M. pendula* and **F** *Mycoplasma* ASV S1 in *S. exserta* along longitude. Samples where zero reads were detected are represented with open circles. **G** Barplots showing the five most abundant ASVs that differed between sites in *P. biscaya*

pendula from western sites (Fig. 4B, D, ANCOM-BC, $9 \times 10^{-11} \leq q \leq 0.03$). Similarly, *Ca. Marinoplasma* and other photosynthetic taxa including several chloroplast ASVs were more abundant in the west. Notably, two ASVs classified as *Prochloron* comprised over 50% of the microbial community in some corals from adjacent sites in the west (Fig. 4B). Only two ASVs associated with *S. exserta* were significantly more abundant in the west including an unclassified gamma-proteobacterium (Fig. S3G in Additional File 1; ANCOM-BC q = 0.0018) and the dominant *Mycoplasma* ASV S1 which was completely absent from all samples from the three easternmost sites (Fig. 4F; q = 4×10^{-19}).

Remaining site scale microbiome variation

The abundances of many microbial taxa were not correlated with depth nor longitude but still differed across sites. These comprised up to 54% of the community in *M. pendula* and 36% in *S. exserta.* Many ASVs were only detected in colonies from a few sites or even a single site. Examples include three close relatives of *Endozoicomonas* averaging a total relative abundance of 26% in *M. pendula* at McNeil bank (Fig. S3E in Additional File 1) and potential parasites within *Rickettsiales* in all coral species. Other examples include a corallicolid ASV only detected in *C. delta* colonies from VK826, GC234, and MC885 and another corallicolid ASV only detected in colonies from GC234 (Fig. S3H, I in Additional File 1).

In *P. biscaya,* the most abundant ASVs differed substantially across sites but did not correlate strongly with depth or longitude (Fig. 4G). For instance, SUP05 had a high abundance in colonies from GC852, *Endozoicomonas* ASV P1 was abundant at DC673 and KC405, *Pseudoalteromonas* ASV P1 was abundant at MC297, and *Mycoplasma* ASV P1 was abundant at most sites but its mean relative abundance ranged from 0.1 to 74% across sites.

Discussion

Differences between coral species

Coral species was the strongest factor differentiating microbial communities. Species differed markedly in which microbes they associated with and also the diversity of their microbial communities. Variants of shared taxa such as *Endozoicomonas* and *Mycoplasma* were species-specific suggesting possible adaptation to different coral hosts. Other dominant microbes belonged to different phyla, such as BD1-7 in *S. exserta* and *Ca. Oceanoplasma* in *C. delta,* suggesting that the metabolic function of microbial associates may differ between coral species.

Microbiome diversity differed strongly across coral species which may reflect different ecological strategies

[82]. Some corals like *M. pendula* and *P. biscaya* appear to be microbial generalists that foster more diverse and flexible microbial communities. In contrast, other corals like *S. exserta* and *C. delta* appear to have specialized communities that are less diverse and less variable [82, 83]. Alternatively, *S. exserta* and *C. delta* may have higher absolute abundances of their dominant associates reducing the richness and evenness of their communities. Measuring absolute microbial abundances would aid the interpretation of differences in richness and evenness between species. For example, *Endozoicomonas* dropped in relative abundance in a Mediterranean coral in response to a heatwave, but this was shown to be due to the growth of opportunistic bacteria while the absolute abundance of *Endozoicomonas* remained the same [84].

These comparisons between species rely on the wide sampling range of this study. *M. pendula* and *P. biscaya* had the highest microbial diversities and greater variation across sites (Fig. S1 in Additional File 1). However, at some sites their diversities were comparable to both *S. exserta* and *C. delta.* This demonstrates the importance of sampling widely across a host species' range in order to fully assess microbial diversity.

The influence of depth

Depth strongly structured the microbial communities of all coral species investigated. We observed differences in the composition, diversity, and abundance of specific microbial ASVs and families. The number and variety of taxon-specific patterns with depth reflect the likelihood that depth structures microbial communities through multiple mechanisms.

For instance, some variation in microbial communities may be due to temperature which decreases from > 30 °C at the surface to 4 °C below ~ 1500 m in the Gulf of Mexico. Depth and temperature were correlated with community composition in coral species living shallower than 1500 m. Previous studies have shown that shallow-water, scleractinian corals from locations with different temperature regimes host different microbial communities [45, 85]. Specifically, the stress of high temperatures shapes corals' microbiomes [86], especially if they bleach [87–90]. The corals in our study may experience different frequencies or intensities of thermally induced stress which may influence their microbiomes. While temperature may be the underlying cause of some of the variation with depth, it does not appear to be the only factor.

The genetic divergence of coral populations may further contribute to differentiation in microbial communities across depths. In the scleractinian *Pocillopora damicornis,* genetically distinct coral populations harbor distinct microbial communities [40]. The turnover of the *Shewanella* community in *C. delta* is consistent with its

population genetic structure [60, 61]. Coral colonies from the deepest two sites were genetically distinct and hosted unique *Shewanella* communities. Thus, some of the differentiation in microbial communities across depth may be caused by genetic differentiation of the coral host.

Other patterns with depth appear to be driven by different causes. For instance, the diversity of microbial associates of *M. pendula* decreased continuously with depth and may be due to a decrease in bacterioplankton (Fig. 2E, F). Indeed, some bacteria from mostly free-living taxa decreased in abundance with depth in *M. pendula* including Colwelliaceae and Marinobacteraceae. Further, light intensity may play a role since photosynthetic taxa associated with *M. pendula* predictably decreased with depth.

Many symbiotic taxa differed in abundance with depth such as *Endozoicomonas, Mycoplasma,* and corallicolids. However, the reasons for this are unclear because many of these microbe's roles and interactions with their coral hosts are unknown or not well-characterized. Interestingly, corallicolids increased in abundance with depth in both *M. pendula* and *S. exserta,* but no depth pattern was found in corallicolids that infect *C. delta.* This is in contrast to previous studies that found a decrease in abundance with depth in the shallow-water coral, *Montastraea annularis,* and across dozens of species spanning a depth of 2 km [9, 91]. These inconsistencies may be explained if corallicolids, like their close relatives, infect intermediate hosts with differing depth distributions. Some of the closest relatives of corallicolids are found in fish [92–94], opening the possibility that corallicolids may use fish as intermediate hosts and could be limited by their depth ranges.

Altogether, depth may structure microbial communities through multiple mechanisms, including changes in free-living microbial communities, decreasing light levels, and genetic differentiation of host corals. When comparing different coral species, a recent review found that octocoral and scleractinian species from shallow water had more diverse microbial communities than their relatives from deeper depths [95]. This suggests that some of these mechanisms may influence microbial community structure on greater scales.

Variation across geography

In addition to variation across depth, we found that the microbial communities of all four species differed geographically. Corals from different sites differed strongly in microbial communities in all species. Yet nearby sites showed similarities reflecting regional-scale geographic variation.

Regional scale variation was identified in both mesophotic coral species. Both *M. pendula* and *S. exserta* had higher diversity in eastern sites where many likely free-living microbial taxa were detected at higher abundances. This may be due to the influence of the Mississippi River on bacterioplankton. There are marked longitudinal differences in surface primary productivity in the northern Gulf of Mexico, being higher in the area of influence of the Mississippi River. Microbial communities of shallow-water corals appear to be significantly influenced by surface primary productivity [96]. This is consistent with our observation that octocoral microbiomes were significantly correlated with surface primary productivity.

Symbiotic taxa also differed in abundance regionally including *Endozoicomonas,* Mollicutes, and corallicolids. This is consistent with other studies that found geographic variation in *Endozoicomonas* and *Mycoplasma* associates in shallow-water corals [15, 20]. Some of the regional patterns may result from limited dispersal since some ASVs were restricted to nearby sites like *Mycoplasma* ASV S1, which was completely absent in all *S. exserta* colonies from the three easternmost sites.

For every coral species, microbial communities differed strongly between sites after accounting for depth and geographic region. This is likely due to additional differences in local environmental conditions between sites that influence microbial community structure. For instance, the high abundance of the SUP05 cluster in *P. biscaya* at GC852 may reflect the presence of seeps nearby [97] (< 450 m). Similarly, the abundance of *Pseudoalteromonas* in *P. biscaya* at the Mississippi Canyon sites may reflect the lasting impact of the Deepwater Horizon oil spill [55, 65, 98]. Consistent deviations from depth trends at certain sites suggest that other factors play a role. For example, the total corallicolid abundance in *M. pendula* at Roughtongue Reef was higher than expected given the trend with depth (Fig. 3B). Conversely, corals from some subsets of sites displayed similar microbial communities despite being far apart and inhabiting different depths. For instance, *P. biscaya* from KC405 and DC673 were dominated by *Endozoicomonas* ASV P1, but it comprised no more than 0.12% in any colony from any other site. These sites are the farthest apart of all sites and do not have overlapping depths. Interestingly, coral populations from these two sites are closely related [62] suggesting an influence of the coral host's genotype on the presence of *Endozoicomonas.*

Implications for restoration efforts

Characterizations of coral microbiomes based on samples from a single site or even a few sites may miss substantial variation across a species' range. This is important to consider in restoration plans that utilize collections from different locations. For example, a restoration plan could use this information to avoid inadvertently transmitting

parasites to new sites through transplants or to avoid rearing infected and non-infected corals together in aquaria. Examples of geographic variation in potential parasites discovered in this work include corallicolids in *C. delta* at VK826, MC885, and GC234 and the unique corallicolids in *M. pendula* and *S. exserta* at Elvers Bank.

Considerations for microbial taxa at low abundance

Some methodological factors may have influenced the patterns among microbial taxa at low relative abundances therefore these should be interpreted carefully. Low levels of contamination between samples cannot be ruled out. In some instance, multiple coral samples were collected in the same container, sometimes involving different species. However, all corals were transferred to fresh seawater individually before preservation. Also, all samples were sequenced on the same lane allowing for potential sample bleeding [99]. Because of these considerations, this manuscript focused on patterns involving microbes with high relative abundance.

Conclusions

This work characterizes the microbial communities of four dominant coral species in the Gulf of Mexico and demonstrates substantial variability across their ranges. These results provide promising targets to study the interactions between corals and their associated microbes. They also reveal substantial variability associated with depth and geography that could only be uncovered through extensive sampling across the hosts' range. The numerous patterns associated with depth demonstrate that in addition to its ecological and evolutionary effects on corals, it also strongly structures their microbial communities.

Abbreviations

ASV	Amplicon sequence variant
RADseq	Restriction site-associated DNA sequence
MLR	Multiple linear regression
PERMANOVA	Permutational multivariate analysis of variance
db-RDA	Distance-based redundancy analysis
MRM	Multiple regression on distance matrices
ANCOM-BC	Analysis of composition of microbiomes with bias correction

Supplementary Information

The online version contains supplementary material available at https://doi.org/10.1186/s40793-024-00579-0.

> Additional file1: Supplementary information including supplementary methods and results. Fig. S1 shows richness and evenness by coral by site. Fig S2 shows additional patterns with depth. Fig S3 shows additional patterns with longitude and site. Figs S4–S7 show correlation plots of environmental variables for all four coral species. Fig S8 shows principal coordinates analyses (PCoA) of each species individually showing differences across sites. (PDF 2395 KB)
>
> Additional file2: Table S1 presents all sample metadata. Table S2 presents all environmental variables by site. Table S3 provides explanations for which variables were included in models. Table S4 presents results from PERMANOVA analyses. Table S5 presents results from db-RDA analyses. Table S6 reports dominant and core ASVs. Table S7 presents results from all analyses on richness and evenness. Table S8 presents results using genetic data. Table S9 presents analyses investigating the effect of preservation method and sampling year. Table S10 presents results comparing this study to a similar dataset. Table S11 provides an analysis of homogeneity of multivariate dispersions for each species based on site. Table S12 displays additional analyses. (XLSX 211 KB)
>
> Additional file3: Contains all results from ANCOM-BC tests. (XLSX 4985 KB)
>
> Additional file4: Contains information from comparison dataset. Includes sample metadata, ASV table, taxonomy of ASVs, and ANCOM-BC results for Callogorgia delta samples. (XLSX 2950 KB)

Author contributions

SAV conceptualized the study, collected samples, conducted fieldwork, conducted analyses, and wrote the manuscript. SH conceptualized the study, secured funding, conducted and led fieldwork, collected samples, conducted analyses, and edited the manuscript.

Availability of data and materials

The sequence read datasets generated and analyzed during the current study are available in the NCBI Sequence Read Archive (SRA) database (www.ncbi.nlm.nih.gov/sra) under Bioproject numbers PRJNA875098 (16S amplicon) and PRJNA821014, PRJNA821015, PRJNA821012, and PRJNA766840 (RADseq). Commands used to process sequence data and R code used for statistical analyses are available on FigShare at https://doi.org/10.6084/m9.figshare.23656992.v1 and https://doi.org/10.6084/m9.figshare.21713954.v1.

Declarations

Ethics approval and consent to participate

Collections in the Flower Garden Banks National Marine Sanctuary were approved under permits FGBNMS-2017-007-A2 and FGBNMS-2019-003-A2. Sampling octocorals in the Gulf of Mexico outside of this area does not require permits.

Consent for publication

Not applicable.

Competing interests

The authors declare no competing interests.

References

1. Pollock FJ, McMinds R, Smith S, Bourne DG, Willis BL, Medina M, et al. Coral-associated bacteria demonstrate phylosymbiosis and cophylogeny. Nat Commun. 2018;9:4921.
2. Siboni N, Ben-Dov E, Sivan A, Kushmaro A. Global distribution and diversity of coral-associated Archaea and their possible role in the coral holobiont nitrogen cycle. Environ Microbiol. 2008;10:2979–90.
3. Wegley L, Yu Y, Breitbart M, Casas V, Kline DI, Rohwer F. Coral-associated archaea. Mar Ecol Prog Ser. 2004;273:89–96.
4. Ainsworth T, Fordyce A, Camp E. The other microeukaryotes of the coral reef microbiome. Trends Microbiol. 2017;25:980–91.
5. Thurber RV, Payet JP, Thurber AR, Correa A. Virus–host interactions and their roles in coral reef health and disease. Nat Rev Microbiol. 2017;15:205–16.
6. Klinges G, Maher RL, Vega Thurber RL, Muller EM. Parasitic '*Candidatus Aquarickettsia rohweri*' is a marker of disease susceptibility in *Acropora cervicornis* but is lost during thermal stress. Environ Microbiol. 2020;22:5341–55.
7. Lesser MP, Falcón LI, Rodríguez-Román A, Enríquez S, Hoegh-Guldberg O, Iglesias-Prieto R. Nitrogen fixation by symbiotic cyanobacteria provides a source of nitrogen for the scleractinian coral *Montastraea cavernosa*. Mar Ecol Prog Ser. 2007;346**:**143–152.
8. Lesser MP, Mazel CH, Gorbunov MY, Falkowski PG. Discovery of symbiotic nitrogen-fixing cyanobacteria in corals. Science. 2004;305:997–1000.
9. Vohsen SA, Anderson KE, Gade AM, Gruber-Vodicka HR, Dannenberg RP, Osman EO, et al. Deep-sea corals provide new insight into the ecology, evolution, and the role of plastids in widespread apicomplexan symbionts of anthozoans. Microbiome. 2020;8:34.
10. Kwong WK, del Campo J, Mathur V, Vermeij MJA, Keeling PJ. A widespread coral-infecting apicomplexan with chlorophyll biosynthesis genes. Nature. 2019;568:103–7.
11. Mathur V, del Campo J, Kolisko M, Keeling PJ. Global diversity and distribution of close relatives of apicomplexan parasites. Environ Microbiol. 2018;20:2824–33.
12. Kirk NL, Ritson-Williams R, Coffroth MA, Miller MW, Fogarty ND, Santos SR. Tracking transmission of apicomplexan symbionts in diverse caribbean corals. PLoS ONE. 2013;8:10.
13. Kirk NL, Thornhill DJ, Kemp DW, Fitt WK, Santos SR. Ubiquitous associations and a peak fall prevalence between apicomplexan symbionts and reef corals in Florida and the Bahamas. Coral Reefs. 2013;32:847–58.
14. Weiler BA, Verhoeven JTP, Dufour SC. (2018) Bacterial communities in tissues and surficial mucus of the cold-water coral *Paragorgia arborea*. Front Mar Sci. 5:378.
15. Woo S, Yang S-H, Chen H-J, Tseng Y-F, Hwang S-J, De Palmas S, et al. Geographical variations in bacterial communities associated with soft coral *Scleronephthya gracillimum*. PLoS ONE. 2017;12: e0183663.
16. Holm JB, Heidelberg KB. Microbiomes of *Muricea californica* and *M. fruticosa*: comparative analyses of two co-occurring Eastern Pacific octocorals**.** Front Microbiol. 2016;7.
17. Kellogg CA, Lisle JT, Galkiewicz JP. Culture-independent characterization of bacterial communities associated with the cold-water coral *Lophelia pertusa* in the Northeastern Gulf of Mexico. Appl Environ Microbiol. 2009;75:2294–303.
18. Neulinger SC, Gärtner A, Järnegren J, Ludvigsen M, Lochte K, Dullo W-C. Tissue-associated, "*Candidatus Mycoplasma corallicola*" and filamentous bacteria on the cold-water coral *Lophelia pertusa* (Scleractinia**)**. Appl Environ Microbiol. 2009;75:1437–44.
19. Gray MA, Stone RP, McLaughlin MR, Kellogg CA. Microbial consortia of gorgonian corals from the Aleutian Islands. FEMS Microbiol Ecol. 2011;76:109–20.
20. Neave MJ, Rachmawati R, Xun L, Michell CT, Bourne DG, Apprill A, et al. Differential specificity between closely related corals and abundant *Endozoicomonas* endosymbionts across global scales. ISME J. 2017;11:186–200.
21. van de Water JAJM, Voolstra CR, Rottier C, Cocito S, Peirano A, Allemand D, et al. Seasonal stability in the microbiomes of temperate gorgonians and the red coral *Corallium rubrum* across the Mediterranean Sea. Microb Ecol. 2018;75:274–288.
22. van de Water JAJM, Melkonian R, Voolstra CR, Junca H, Beraud E, Allemand D, et al. Comparative assessment of Mediterranean gorgonian-associated microbial communities reveals conserved core and locally variant bacteria**.** Microb Ecol. 2017;73:466–478.
23. Bayer T, Neave MJ, Alsheikh-Hussain A, Aranda M, Yum LK, Mincer T, et al. The microbiome of the Red Sea coral *Stylophora pistillata* is dominated by tissue-associated *Endozoicomonas* bacteria. Appl Environ Microbiol. 2013;79:4759–62.
24. La Rivière M, Garel M, Bally M. Localization of endobacteria in the gastrodermis of a Mediterranean gorgonian coral, *Paramuricea clavata*, using fluorescence in situ hybridization. Mar Biol. 2016;163:206.
25. Pogoreutz C, Oakley CA, Rädecker N, Cárdenas A, Perna G, Xiang N, et al. Coral holobiont cues prime *Endozoicomonas* for a symbiotic lifestyle**.** ISME J. 2022:1–13.
26. Neave MJ, Michell CT, Apprill A, Voolstra CR. *Endozoicomonas* genomes reveal functional adaptation and plasticity in bacterial strains symbiotically associated with diverse marine hosts. Sci Rep. 2017;7:40579.
27. Tandon K, Lu C-Y, Chiang P-W, Wada N, Yang S-H, Chan Y-F, et al. Comparative genomics: dominant coral-bacterium *Endozoicomonas acroporae* metabolizes dimethylsulfoniopropionate (DMSP). ISME J. 2020;14:1290–303.
28. Wada N, Hsu M-T, Tandon K, Hsiao SS-Y, Chen H-J, Chen Y-H, et al. High-resolution spatial and genomic characterization of coral-associated microbial aggregates in the coral *Stylophora pistillata*. Sci Adv. 2022;8:eabo2431.
29. Pogoreutz C, Ziegler M. Frenemies on the reef? Resolving the coral–*Endozoicomonas* association**.** Trends Microbiol. 2024;11.
30. Vohsen SA, Gruber-Vodicka HR, Meyer M, Sadowski M, Dubilier N, Fisher CR, et al. Discovery of deep-sea coral symbionts from a novel family of marine bacteria, Oceanoplasmataceae, with severely reduced genomes. bioRxiv. 2022. https://doi.org/10.1101/2022.10.07.511369.
31. Quintanilla E, Ramírez-Portilla C, Adu-Oppong B, Walljasper G, Glaeser SP, Wilke T, et al. Local confinement of disease-related microbiome facilitates recovery of gorgonian sea fans from necrotic-patch disease. Sci Rep. 2018;8:14636.
32. van de Water JAJM, Allemand D, Ferrier-Pagès C. Host-microbe interactions in octocoral holobionts—recent advances and perspectives. Microbiome. 2018;6:64.
33. McCauley M, Jackson CR, Goulet TL. Microbiomes of Caribbean octocorals vary over time but are resistant to environmental change. Front Microbiol. 2020;11:1272.
34. Morrison DA. Evolution of the Apicomplexa: where are we now? Trends Parasitol. 2009;25:375–82.
35. Razin S, Hayflick L. Highlights of mycoplasma research—an historical perspective. Biologicals. 2010;38:183–90.
36. Toller WW, Rowan R, Knowlton N. Genetic evidence for a protozoan (phylum Apicomplexa) associated with corals of the *Montastraea annularis* species complex. Coral Reefs. 2002;21:143–6.
37. Dubé CE, Ziegler M, Mercière A, Boissin E, Planes S, Bourmaud CAF, et al. Naturally occurring fire coral clones demonstrate a genetic and environmental basis of microbiome composition. Nat Commun. 2021;12:6402.
38. van de Water JAJM, Coppari M, Enrichetti F, Ferrier-Pagès C, Bo M. Local conditions influence the prokaryotic communities associated with the mesophotic black coral *Antipathella subpinnata*. Front Microbiol. 2020;11.
39. Durante MK, Baums IB, Williams DE, Vohsen S, Kemp DW. What drives phenotypic divergence among coral clonemates of *Acropora palmata*? Mol Ecol. 2019;28:3208–24.
40. van Oppen MJH, Bongaerts P, Frade P, Peplow Lesa M, Boyd SE, Nim HT, et al. Adaptation to reef habitats through selection on the coral animal and its associated microbiome. Mol Ecol. 2018;27:2956–71.
41. Wang L, Shantz AA, Payet JP, Sharpton TJ, Foster A, Burkepile DE, et al. Corals and their microbiomes are differentially affected by exposure to elevated nutrients and a natural thermal anomaly. Front Mar Sci. 2018;5:16.
42. Roder C, Bayer T, Aranda M, Kruse M, Voolstra CR. Microbiome structure of the fungid coral *Ctenactis echinata* aligns with environmental differences. Mol Ecol. 2015;24:3501–11.
43. Klinges JG, Patel SH, Duke WC, Muller EM, Vega Thurber RL. Phosphate enrichment induces increased dominance of the parasite *Aquarickettsia* in the coral *Acropora cervicornis*. FEMS Microbiol Ecol. 2022**:**fiac013.
44. Dannenberg RP. Characterization and oil response of the deep sea coral-associated microbiome**.** PhD thesis. The Pennsylvania State University,

Biology Department; 2015. https://etda.libraries.psu.edu/files/final_submissions/11614.

45. Osman EO, Suggett DJ, Voolstra CR, Pettay DT, Clark DR, Pogoreutz C, et al. Coral microbiome composition along the northern Red Sea suggests high plasticity of bacterial and specificity of endosymbiotic dinoflagellate communities. Microbiome. 2020;8:1–16.

46. Osman EO, Smith DJ, Ziegler M, Kürten B, Conrad C, El-Haddad KM, et al. Thermal refugia against coral bleaching throughout the northern Red Sea. Glob Change Biol. 2018;24:e474–84.

47. Rosado PM, Leite DCA, Duarte GAS, Chaloub RM, Jospin G, Nunes da Rocha U, et al. Marine probiotics: increasing coral resistance to bleaching through microbiome manipulation. ISME J. 2019;13:921–936.

48. Roberts JM, Wheeler AJ, Freiwald A, Cairns SD. Cold-water corals the biology and geology of deep-sea coral habitats. New York: Cambridge University Press; 2009.

49. Jensen A, Frederiksen R. The fauna associated with the bank-forming deepwater coral *Lophelia pertusa* (Scleractinaria) on the Faroe shelf. Sarsia. 1992;77:53–69.

50. Buhl-Mortensen L, Mortensen PB. Distribution and diversity of species associated with deep-sea gorgonian corals off atlantic Canada. In: Freiwald A, Roberts JM, editors. Cold-water corals and ecosystems. Berlin, Heidelberg: Springer; 2005. p. 849–79.

51. Sinniger F, Ballantine D, Bejarano I, Colin P, Pochon X, Pomponi S, et al. Biodiversity of mesophotic coral ecosystems. In: Baker EK, Puglise KA, Harris PT, editors, Mesophotic coral ecosystems—a lifeboat for coral reefs? United Nations Environment Programme; 2016. p. 50–62.

52. Pinheiro H, Goodbody-Gringley G, Jessup M, Shepherd B, Chequer A, Rocha L. Upper and lower mesophotic coral reef fish communities evaluated by underwater visual censuses in two Caribbean locations. Coral Reefs. 2016;35:139–51.

53. Henderson MJ, Huff DD, Yoklavich MM. Deep-sea coral and sponge taxa increase demersal fish diversity and the probability of fish presence. Front Mar Sci. 2020;7: 593844.

54. Silva M, Etnoyer PJ, MacDonald IR. Coral injuries observed at mesophotic reefs after the Deepwater Horizon oil discharge. Deep Sea Res Part II Top Stud Oceanogr. 2016;129:96–107.

55. White HK, Hsing PY, Cho W, Shank TM, Cordes EE, Quattrini AM, et al. Impact of the Deepwater Horizon oil spill on a deep-water coral community in the Gulf of Mexico. Proc Natl Acad Sci USA. 2012;109:20303–8.

56. Guinotte JM, Orr J, Cairns S, Freiwald A, Morgan L, George R. Will human-induced changes in seawater chemistry alter the distribution of deep-sea scleractinian corals? Front Ecol Environ. 2006;4:141–6.

57. Hoegh-Guldberg O, Poloczanska ES, Skirving W, Dove S. Coral reef ecosystems under climate change and ocean acidification. Front Mar Sci. 2017;4:158.

58. Cairns SD. Deep-water corals: an overview with special reference to diversity and distribution of deep-water scleractinian corals. Bull Mar Sci. 2007;81:311–22.

59. Yesson C, Taylor ML, Tittensor DP, Davies AJ, Guinotte J, Baco A, et al. Global habitat suitability of cold-water octocorals. J Biogeogr. 2012;39:1278–92.

60. Quattrini AM, Baums IB, Shank TM, Morrison CL, Cordes EE. Testing the depth-differentiation hypothesis in a deepwater octocoral. Proc Royal Soc B. 2015;282:20150008.

61. Bracco A, Liu G, Galaska MP, Quattrini AM, Herrera S. Integrating physical circulation models and genetic approaches to investigate population connectivity in deep-sea corals. J Mar Syst. 2019;198: 103189.

62. Galaska MP, Liu G, West D, Erickson K, Quattrini AM, Bracco A, et al. Seascape genomics reveals metapopulation connectivity network of *Paramuricea biscaya* in the northern Gulf of Mexico. Front Mar Sci. 2021;1790.

63. Rex MA, Etter RJ. Deep-sea biodiversity: pattern and scale. Harvard University Press; 2010.

64. Etnoyer PJ, Wickes LN, Silva M, Dubick J, Balthis L, Salgado E, et al. Decline in condition of gorgonian octocorals on mesophotic reefs in the northern Gulf of Mexico: before and after the Deepwater Horizon oil spill. Coral Reefs. 2016;35:77–90.

65. Fisher CR, Hsing P-Y, Kaiser CL, Yoerger DR, Roberts HH, Shedd WW, et al. Footprint of *Deepwater Horizon* blowout impact to deep-water coral communities. Proc Natl Acad Sci USA. 2014;111:11744–9.

66. Quattrini AM, Georgian SE, Byrnes L, Stevens A, Falco R, Cordes EE. Niche divergence by deep-sea octocorals in the genus *Callogorgia* across the continental slope of the Gulf of Mexico. Mol Ecol. 2013;22:4123–40.

67. Herrera S. Salting-out protocol for extracting hmw genomic DNA from frozen octocorals. protocols.io. 2022. https://doi.org/10.17504/protocols.io.bypypvpw Accessed 24 January 2024.

68. Naqib A, Poggi S, Wang W, Hyde M, Kunstman K, Green SJ. Making and sequencing heavily multiplexed, high-throughput 16S ribosomal RNA gene amplicon libraries using a flexible, two-stage PCR protocol. In: Raghavachari N, Garcia-Reyero N, editors. Gene Expression Analysis: Methods and Protocols. New York: Humana Press; 2018. p. 149–169. [Walker JM (Series Editor): Methods in Molecular Biology].

69. Bolyen E, Rideout JR, Dillon MR, Bokulich NA, Abnet C, Al-Ghalith GA, et al. QIIME 2: Reproducible, interactive, scalable, and extensible microbiome data science. PeerJ Prepr. 2018;6:e27295v27292.

70. Catchen J, Hohenlohe PA, Bassham S, Amores A, Cresko WA. Stacks: an analysis tool set for population genomics. Mol Ecol. 2013;22:3124–40.

71. Parra-Salazar A, Gomez J, Lozano-Arce D, Reyes-Herrera PH, Duitama J. Robust and efficient software for reference-free genomic diversity analysis of genotyping-by-sequencing data on diploid and polyploid species. Mol Ecol Resour. 2022;22:439–54.

72. Kamvar ZN, Tabima JF, Grünwald NJ. Poppr: an R package for genetic analysis of populations with clonal, partially clonal, and/or sexual reproduction. PeerJ. 2014;2: e281.

73. Dray S, Dufour A-B. The ade4 package: implementing the duality diagram for ecologists. J Stat Softw. 2007;22:1–20.

74. McInnes L, Healy J, Melville J. Umap: Uniform manifold approximation and projection for dimension reduction. arXiv. 2018. https://doi.org/10.48550/arXiv.1802.03426.

75. Dixon P. VEGAN, a package of R functions for community ecology. J Veg Sci. 2003;14:927–30.

76. Hurlbert SH. The nonconcept of species diversity: a critique and alternative parameters. Ecology. 1971;52:577–86.

77. Lahti L, Shetty S. Introduction to the microbiome r package. 2018. https://microbiome.github.io/tutorials/. Accessed 24 January 2024

78. Anderson MJ. Permutational multivariate analysis of variance (PERMANOVA). In: Kenett RS, Longford NT, Piegorsch WW, Ruggeri F, editors. Wiley StatsRef: Statistics Reference Online. 2017. p. 1–15. https://doi.org/10.1002/9781118445112.stat07841

79. Legendre P, Anderson MJ. Distance-based redundancy analysis: testing multispecies responses in multifactorial ecological experiments. Ecol Monogr. 1999;69:1–24.

80. Lichstein JW. Multiple regression on distance matrices: a multivariate spatial analysis tool. Plant Ecol. 2007;188:117–31.

81. Lin H, Peddada SD. Analysis of compositions of microbiomes with bias correction. Nat Commun. 2020;11:3514.

82. Voolstra CR, Ziegler M. Adapting with microbial help: microbiome flexibility facilitates rapid responses to environmental change. BioEssays. 2020;42:2000004.

83. Ziegler M, Grupstra CGB, Barreto MM, Eaton M, BaOmar J, Zubier K, et al. Coral bacterial community structure responds to environmental change in a host-specific manner. Nat Commun. 2019;10:3092.

84. Prioux C, Tignat-Perrier R, Gervais O, Estaque T, Schull Q, Reynaud S, et al. Unveiling microbiome changes in Mediterranean octocorals during the 2022 marine heatwaves: quantifying key bacterial symbionts and potential pathogens. Microbiome. 2023;11:271.

85. Lima LF, Weissman M, Reed M, Papudeshi B, Alker AT, Morris MM, et al. Modeling of the coral microbiome: the influence of temperature and microbial network. MBio. 2020;11:e02691-e12619.

86. Lee STM, Davy SK, Tang S-L, Fan T-Y, Kench PS. Successive shifts in the microbial community of the surface mucus layer and tissues of the coral *Acropora muricata* under thermal stress. FEMS Microbiol Ecol. 2015;91.

87. Ziegler M, Seneca FO, Yum LK, Palumbi SR, Voolstra CR. Bacterial community dynamics are linked to patterns of coral heat tolerance. Nat Commun. 2017;8:14213.

88. Pootakham W, Mhuantong W, Yoocha T, Putchim L, Jomchai N, Sonthirod C, et al. Heat-induced shift in coral microbiome reveals several members of the Rhodobacteraceae family as indicator species for thermal stress in *Porites lutea*. MicrobiologyOpen. 2019;8: e935.

89. Bourne D, Iida Y, Uthicke S, Smith-Keune C. Changes in coral-associated microbial communities during a bleaching event. ISME J. 2008;2:350–63.

90. Grottoli AG, Dalcin Martins P, Wilkins MJ, Johnston MD, Warner ME, Cai W-J, et al. Coral physiology and microbiome dynamics under combined warming and ocean acidification. PLoS ONE. 2018;13: e0191156.
91. Klaus JS, Janse I, Heikoop JM, Sanford RA, Fouke BW. Coral microbial communities, zooxanthellae and mucus along gradients of seawater depth and coastal pollution. Environ Microbiol. 2007;9:1291–305.
92. Sikkel PC, Cook CA, Renoux LP, Bennett CL, Tuttle LJ, Smit NJ. The distribution and host-association of a haemoparasite of damselfishes (Pomacentridae) from the eastern Caribbean based on a combination of morphology and 18S rDNA sequences. Int J Parasitol Parasites Wildl. 2018;7:213–20.
93. Janouškovec J, Tikhonenkov DV, Burki F, Howe AT, Kolisko M, Mylnikov AP, et al. Factors mediating plastid dependency and the origins of parasitism in apicomplexans and their close relatives. Proc Natl Acad Sci USA. 2015;112:10200–7.
94. Janouškovec J, Horák A, Barott KL, Rohwer FL, Keeling PJ. Global analysis of plastid diversity reveals apicomplexan-related lineages in coral reefs. Curr Biol. 2012;22:R518–9.
95. McCauley M, Goulet T, Jackson C, Loesgen S. Systematic review of cnidarian microbiomes reveals insights into the structure, specificity, and fidelity of marine associations. Nat Commun. 2023;14:4899.
96. Glasl B, Bourne DG, Frade PR, Thomas T, Schaffelke B, Webster NS. Microbial indicators of environmental perturbations in coral reef ecosystems. Microbiome. 2019;7:1–13.
97. Feng D, Cordes EE, Roberts HH, Fisher CR. A comparative study of authigenic carbonates from mussel and tubeworm environments: implications for discriminating the effects of tubeworms. Deep Sea Res Part I Oceanogr Res Pap. 2013;75:110–8.
98. Girard F, Fisher CR. Long-term impact of the Deepwater Horizon oil spill on deep-sea corals detected after seven years of monitoring. Biol Conserv. 2018;225:117–27.
99. Kircher M, Sawyer S, Meyer M. Double indexing overcomes inaccuracies in multiplex sequencing on the Illumina platform. Nucleic Acids Res. 2012;40:e3–e3.

Publisher's Note